Cell Signal. Author manuscript; available in PMC 2013 July 11.

Published in final edited form as:
Cell Signal. 2011 December ; 23(12): 2030–2038. doi:10.1016/j.cellsig.2011.07.017.

Bcl-xL phosphorylation at Ser49 by polo kinase 3 during cell cycle progression and checkpoints

Jianfang Wang[a], **Myriam Beauchemin**[a], and **Richard Bertrand**[a,b,*]

[a]Centre de recherche, Centre hospitalier de l'Université de Montréal (CRCHUM), Hôpital Notre-Dame and Institut du cancer de Montréal, Montréal, Québec, Canada

[b]Département de médecine, Université de Montréal, Montréal, Québec, Canada

Abstract

Functional analysis of a Bcl-xL phosphorylation mutant series has revealed that cells expressing Bcl-xL(Ser49Ala) mutant are less stable at G2 checkpoint after DNA damage and enter cytokinesis more slowly after microtubule poisoning, than cells expressing wild-type Bcl-xL. These effects of Bcl-xL(Ser49Ala) mutant seem to be separable from Bcl-xL function in apoptosis. Bcl-xL(Ser49) phosphorylation is cell cycle-dependent. In synchronized cells, phospho-Bcl-xL(Ser49) appears during the S phase and G2, whereas it disappears rapidly in early mitosis during prometaphase, metaphase and early anaphase, and re-appears during telophase and cytokinesis. During DNA damage-induced G2 arrest, an important pool of phospho-Bcl-xL(Ser49) accumulates in centrosomes which act as essential decision centers for progression from G2 to mitosis. During telophase/cytokinesis, phospho-Bcl-xL (Ser49) is found with dynein motor protein. In a series of in vitro kinase assays, specific small interfering RNA and pharmacological inhibition experiments, polo kinase 3 (PLK3) was implicated in Bcl-xL(Ser49) phosphorylation. These data indicate that, during G2 checkpoint, phospho-Bcl-xL(Ser49) is another downstream target of PLK3, acting to stabilize G2 arrest. Bcl-xL phosphorylation at Ser49 also correlates with essential PLK3 activity and function, enabling cytokinesis and mitotic exit.

Keywords

Bcl-xL; PLK3; Cell cycle; G2 arrest; Cytokinesis; Mitotic exit

[*]Corresponding author at: CRCHUM, Hôpital Notre-Dame and Institut du cancer de Montréal, 1560 Sherbrooke St. East, Room Y-5634, Montréal, Québec, Canada H2L 4M1. Tel.: +1 514 890 8000x26615; fax: +1 514 412 7591. richard.bertrand@umontreal.ca (R. Bertrand).

Online supplemental materials
Supplemental materials for this article, including supplemental figures and tables, are available on the *Cellular Signalling* website.

Disclosure of conflicts of interest
The authors declare no potential conflicts of interest.

Authors' contribution
All authors participated in the research and article preparation. All authors read and approved the final manuscript.

1. Introduction

Bcl-xL (Bcl-2-related gene x, long isoform), a Bcl-2 (B cell leukemia/lymphoma protein-2) family member, is well-characterized for its function in apoptosis [1]. Regulation of outer mitochondrial membrane permeabilization is the major way in which Bcl-xL protein exerts its anti-apoptosis regulatory and survival effect, which means preserving mitochondrial membrane integrity, mitochondrial transmembrane potential as well as ATP production, and preventing the release of apoptogenic factors in cytosol (reviewed in [2–4]). Elucidation of Bcl-xL's 3-dimensional structure has provided a first structural model in which α-helices located in BH1 (Bcl-2 homology domain), BH2 and BH3 domains create an elongated hydrophobic pocket domain where a BH3 amphipathic α-helice of another Bcl-2-like protein can bind [5–7]. Bcl-xL binds to pro-apoptotic family members through protein–protein interactions, forming a complex dynamic network of hetero-oligomers, depending on the cellular environment, stress condition and their subcellular localization [8–13]. Heterodimerization between pro- and anti-apoptotic molecules controls cell fate, indicating that the relative concentration of one faction versus the other greatly influences the susceptibility of cells to death signals (reviewed in [14,15]). BH3-only proteins are potent mediators of cell death. A subset, referred to as BH3-only enabler or sensitizing proteins, promotes apoptosis by binding to and inhibiting pro-survival molecules, such as Bcl-2, Bcl-xL and Mcl-1, whereas BH3-only activator or activating proteins bind to and activate multidomain pro-apoptotic Bax and Bak proteins [10,16]. Bax insertion and oligomerization into membranes require activation, i.e. structural reorganization by a BH3-only activating protein, events that lead to outer mitochondrial membrane permeabilization; in contrast, the ability of anti-apoptotic proteins, such as Bcl-xL, to trap and inhibit these BH3-only activating proteins, prevents membrane permeabilization [17–20].

The unexpected pore-forming ability of Bcl-xL protein has emerged from unfolding of its 3-dimensional structure. Structural similarities between Bcl-xL, particularly its α5- and α6-helices and the pore-forming domains of some bacterial toxins that act as channels for either ions or proteins, suggest that Bcl-2 members could function by constituting pores in intracellular organelles, including mitochondria [5,17–21]. Whether these channel activities function by themselves, or in association with other megachannels, such as components of mitochondrial permeability transition pores, or others, is still not completely elucidated [3,4,19,22–31].

Several studies have revealed that, in addition to their key role in controlling apoptosis, some Bcl-2 family members interface with the cell cycle, DNA damage responses and repair pathways, functions that are distinct from their role in apoptosis (reviewed in [32,33]). Indeed, Bcl-xL and/or Bcl-2 modulate the homologous recombination pathway as well as non-homologous end-joining and DNA damage mismatch repair activities, effects that are separable from their anti-apoptotic task [34–37]. Bcl-xL also fulfills functions during the cell cycle [38–40]. Bcl-xL phosphorylation at Ser62, within the unstructured loop domain of the protein, has been detected most often in cells treated with microtubule poisons, including nocodazole, paclitaxel, vinblastine, vincristine, colchicine and pironetin [41–49], and coupled, more recently, with specific G2 and mitotic events (Wang et al., 2011; manuscripts

submitted). Similarly, Bcl-xL phosphorylation at Thr47 and Thr115 has been documented in response to genotoxic stress induced by ionizing radiation [50].

A previous study in our laboratory showed that Bcl-xL stabilizes the G2 checkpoint, an activity that resides within a specific region between the 41st amino acid and the 60th amino acid included in the flexible loop domain of Bcl-xL [40], a region that is not essential for its anti-apoptotic function [42,51,52]. To search for potentially important phosphorylation site(s) regulating Bcl-xL's function during the cell cycle, we generated and monitored the effects of a series of single-point Bcl-xL phosphorylation mutants within its unstructured loop domain. Taking a variety of experimental approaches with stably-transfected human cell populations and non-transfected wild-type (wt) cells, we now provide evidence that within the unstructured loop domain, Bcl-xL(Ser49) phosphorylation is a key element regulating Bcl-xL's functions at the G2 cell cycle checkpoint and entry into cytokinesis, influencing mitotic exit.

2. Materials and methods

2.1. Cell culture, cDNA construction, cell analysis and statistics

Human Namalwa and HeLa cell lines were obtained from the American Type Culture Collection and grown at 37 °C under 5% CO_2 in RPMI-1640 medium and DMEM supplemented with 10% heat-inactivated fetal bovine serum (FBS), 100 U/ml penicillin and 100 μg/ml streptomycin, respectively. The phosphorylation mutant pCEP4-HA-Bcl-xL(Ser49Ala) was generated by triple polymerase chain reactions (PCR) with wt pCEP4-HA-Bcl-xL vector as DNA template. Briefly, the first fragments were amplified by *Vent* polymerase, with specific adapter primers containing restriction site sequences at the ATG start codon and anti-sense junction primers circumscribing the mutated codon with flanking sequences. The second fragments were amplified by *Vent* polymerase, with sense junction primers containing the mutated codon, with flanking sequences and adapter anti-sense primers comprising restriction site sequences at the TGA stop codon. The 2 amplified fragments were gel-purified, heat-denaturated, and slowly annealed on ice. After elongation by *Taq* polymerase for 10 min, a third PCR, with specific adapter primers containing sequences at the ATG start codon and TGA stop codon, was amplified. The amplified fragment was first cloned in pCR2.1Topo vector (Invitrogen Corporation), sequenced, and then sub-cloned in the eukaryotic expression vector pCEP4 (Invitrogen Corporation). Purified constructs were transfected in Namalwa cells by electroporation at 0.27 kV (Gene Pulser, BioRad, Hercules, CA), and cells were grown under hygromycin B1 selection to attain a stable cell population prior to performing the experiments. Similar procedures were conducted to generate the phosphorylation-mimetic mutant Bcl-xL(Ser49Asp), using as template the pET-Bcl-xL (ΔTM) vector [40]. The kinetics of mitotic entry, cell cycle phase distribution and cell death were monitored in Coulter EpicsXL flow cytometers with phospho-H3(Ser10) labeling and PI staining. HeLa cells were synchronized by double-thymidine block (2 mM) and release. Statistical analyses were performed by standard *Student t-test* with GraphPad Prism software (version 4.0c; San Diego, CA) and $p>0.05$ values were considered as non-significant.

2.2. Protein extraction and immunoblotting

To prepare protein extracts, cells were lysed in buffer containing 20 mM Hepes(KOH), pH 7.4, 120 mM NaCl, 1% Triton X-100, 2 mM phenylmethylsulfonyl fluoride, a cocktail of protease inhibitors (Complete™, Roche Applied Science) and a cocktail of phosphatase inhibitors (PhosStop™, Roche Applied Science). SDS–PAGE were run on 10–18% gradient polyacrylamide gel. The antibodies used in this study are listed in Supplemental Table S2. Bcl-xL(Ser49) antibodies were prepared and purified by GeneScript, using the phosphopeptide-KLH conjugate CTESEMETP(pS)AING as immunogen. The affinity and specificity of the preparations were first analyzed with ELISA, with coated phosphopeptide and non-phosphopeptide as antigens.

2.3. Immunofluorescence microscopy

HeLa cells, seeded and grown directly on coverslips, were fixed in methanol at −20 °C for 30 min and rapidly immersed in ice-cold acetone for a few seconds. The slides were allowed to dry at room temperature and rehydrated in PBS. Nonspecific binding sites were blocked in PBS containing 5% FBS (blocking solution); then, the slides were incubated sequentially with specific primary antibody (10 μg/ml in blocking solution), specific labeled secondary antibody (10 μg/ml in blocking solution), followed by DAPI staining, also performed in blocking solution. Images were generated with a Leica Microsystem mounted on a Leica DM6000B microscope and Leica DFC480 camera hooked up to a Macintosh computer.

2.4. Protein kinase assays and protein kinase chemical inhibitors

The kinases and kinase assays are described in Supplemental Table S3. Enzyme activities were tested on control substrates, and velocities were expressed as nmol/min/mg (data in Supplemental Fig. S2-A–B). Recombinant human Bcl-xL(ΔTM) and Bcl-xL(ΔTM) (Ser49Asp) proteins were produced and purified, as described previously [40]. BI-2536 was obtained from Axon MedChem Corp.

2.5. siRNA-mediated protein kinase inhibition

HeLa cells were transfected with DharmaFECT-1 transfection reagent (ThermoScientific) according to the manufacturer's instructions, with 100 nM of either control siRNA (non-targeting Smart Pool) or siRNA #3 and #4 targeting PLK3 mRNA obtained from Dharmacon, ThermoScientific.

3. Results

3.1. Effect of HA-Bcl-xL and HA-Bcl-xL(Ser49Ala) phosphorylation mutant on G2 checkpoint stability and mitosis progression

First, human B lymphoma Namalwa cells were transfected with expression vectors encoding wt HA-Bcl-xL and HA-Bcl-xL(Ser49Ala) mutant, and stably-transfected cell populations were selected. The protein expression levels are illustrated in Fig. 1A (top right panel). A well-established experimental procedure, referred to as mitotic trap assay [53], evaluated the kinetics of G2 arrest after DNA damage, the kinetics of mitotic entry after G2 arrest, and the kinetics of cell death. In this assay, cells entering mitosis after G2 arrest are trapped by

adding nocodazole (0.35 μM) at 24-h intervals after etoposide (VP16) treatment (10 μM/30 min in Namalwa cells) and monitored by flow cytometry with phospho-H3(Ser10) labeling as well as propidium iodide (PI) staining (Fig. 1A; top left panel). Control Namalwa cells or Namalwa cells stably transfected with empty vector die rapidly after exposure to VP16 (Fig. 1A; green bars). In contrast, cell populations stably expressing wt HA-Bcl-xL and the phosphorylation mutant HA-Bcl-xL(Ser49Ala) show strong inhibition of apoptosis (Fig. 1A; green bars). More than 70% of cells over-expressing wt HA-Bcl-xL are arrested in G2, 24 h after VP16 treatment (Fig. 1A, gray bars), while some cells slowly escape from G2 and enter early mitosis, 36 to 72 h after VP16 (Fig. 1A; red bars). In contrast, cells expressing the phosphorylation mutant HA-Bcl-xL(Ser49Ala) enter mitosis much more rapidly, 36 to 72 h after VP16 (Fig. 1A; red bars), revealing that Ser49 is essential for Bcl-xL's function in G2 arrest. These observations also suggest that Bcl-xL's role in G2 arrest is distinct from its function in apoptosis.

Similar experimental monitoring by flow cytometry with phospho-H3(Ser10) labeling and PI staining was undertaken to evaluate the kinetics of early mitotic entry and stability of the spindle-assembly checkpoint (N4 DNA content, phospho-H3(Ser10)-positive), mitosis progression into cytokinesis (N4 DNA content, phospho-H3(Ser10)-negative, after taxol treatment), G1 entry (N2 DNA content, phospho-H3 (Ser10)-negative), and cell death kinetics (sub-G1 DNA content) in taxol-exposed cells (Fig. 1B). Both Namalwa cells and Namalwa cells stably transfected with empty vector die rapidly after taxol treatment, while cells stably expressing wt HA-Bcl-xL and the phosphorylation mutant HA-Bcl-xL(Ser49Ala) show strong inhibition of apoptosis (Fig. 1B; green bars). Up to 80–85% of cells over-expressing wt HA-Bcl-xL and HA-Bcl-xL(Ser49Ala) mutants accumulate in early mitosis (Fig. 1B; red bars) from 12- to 24-h taxol exposure. Interestingly, HA-Bcl-xL-expressing cells gradually start to lose the phospho-H3(Ser10) marker by 36 h, whereas most HA-Bcl-xL(Ser49Ala) mutant cells are still stable in early mitosis at 36 h, slowly losing the phospho-H3(Ser10) marker only at 48 to 60 h after taxol treatment (Fig. 1B; red bars). These results indicate that Bcl-xL(Ser49) is required for spindle-assembly checkpoint resolution and/or entry into cytokinesis. Again, this effect of Bcl-xL(Ser69Ala) on mitosis progression in taxol-exposed cells appears separable from its anti-apoptotic function.

3.2. Bcl-xL(Ser49) phosphorylation and location during DNA damage-induced G2 arrest and in unpertubed, synchronized wt HeLa cells

First, antibodies were produced to monitor Bcl-xL(Ser49) phosphorylation. The specificity of phospho-Bcl-xL(Ser49) antibodies is depicted in Supplemental Fig. S1. Experiments were then performed in human non-transfected wt HeLa cells, which undergo G2 arrest after VP16 treatment (10 μm; 16 h), with some cells escaping G2 arrest 48 to 72 h post-VP16 treatment (Fig. 2A, right panel). Bcl-xL(Ser49) phosphorylation is observed in wt HeLa cells exposed to VP16 (Fig. 2A, left panel). When wt HeLa cells are synchronized by double thymidine block and released upon progression from S to G2, Bcl-xL is progressively phosphorylated on Ser49 (Fig. 2B, left panel), suggesting that Bcl-xL (Ser49) phosphorylation also occurs during normal cell cycle progression. Cell cycle phase distribution during these experiments is indicated in Fig. 2B, right panel. We next investigated the subcellular location of phospho-Bcl-xL(Ser49) in wt HeLa cells by indirect

immunofluorescence staining, in synchronized G2 control and VP16-induced G2 arrest (Fig. 2C). In HeLa cells exposed to VP16, a pool of phospho-Bcl-xL(Ser49) accumulated in centrosomes with γ-tubulin 24 and 48 h post-VP16 exposure (Fig. 2C). In contrast, no significant accumulation of phospho-Bcl-xL(Ser49) in centrosomes was detected in synchronized, untreated G2 cells (Fig. 2C). Phospho-Bcl-xL(Ser49) was not found in nuclear structures with colin, a specific Cajal body marker, and nucleolin, a specific nucleolus marker (Fig. 2C). Taken together, these results suggest that Bcl-xL is phosphorylated on Ser49 during normal cell cycle progression and that phospho-Bcl-xL(Ser49) accumulates much more strongly in centrosomes during DNA damage-induced G2 checkpoint in HeLa cells. Centrosomes play fundamental roles as organization centers that integrate cell cycle arrest and DNA repair signaling networks in response to genotoxic stress [54]. One important aspect of centrosome biology is the control of cyclin B1/CDK1(CDC2) activity for entry into mitosis [55]. Following DNA damage, premature initiation of mitosis is prevented by inhibiting centrosome-associated cyclin B1/CDK1(CDC2) through CDC25 phosphatase inactivation [56,57]. In HeLa cells treated by VP16, both CDK1(CDC2) and phospho-Bcl-xL(ser49) accumulate in centrosomes during the G2 checkpoint (Supplemental Fig. S2-A). Previous works also have indicated that Bcl-xL co-localized with CDK1 (CDC2) and potently inhibits CDK1(CDC2) kinase activity during the G2 checkpoint [40]. To further investigate the effect of phospho-Bcl-xL (ser49) on CDK1(CDC2) activity, in vitro CDK1(CDC2) kinase assays were performed in the presence of various amounts of purified recombinant Bcl-xL(Ser49Asp) protein lacking its C-terminal hydrophobic transmembrane domain (ΔTM). Bcl-xL(ΔTM)(Ser49Asp) inhibited CDK1(CDC2) activity dose-dependently (Supplemental Fig. S2-B), providing a possible mechanism by which phospho-Bcl-xL(Ser49) exerts its effect on stabilization of the G2 checkpoint.

3.3. Bcl-xL(Ser49) phosphorylation and location during mitosis progression

We next monitored phospho-Bcl-xL(Ser49) during mitosis. First, wt HeLa cells were synchronized by double thymidine block and released upon progression to G2. They were then treated with nocodazole (0.35 μM, 4 h), and prometaphase/metaphase cells were collected by mitotic shake-off. A portion of these cells was released from nocodazole and growth in the presence of MG-132 (25 μM), a proteasome inhibitor that prevents cyclinB1 and securin destruction, to obtain a cell population at the metaphase and anaphase boundary. A second set was also released from nocodazole and by growth in the presence of blebbistatin (10 μM), a selective non-muscle contractile motor myosin II inhibitor that averts furrow ingression, to attain a cell population at telophase/cytokinesis and tetraploid. A schematic view of these experiments appears in Fig. 3A (top panel). Western blotting revealed that Bcl-xL is timely dephosphorylated at Ser49 at prometaphase, metaphase and the anaphase boundary, while it is rapidly phosphorylated at telophase/cytokinesis (Fig. 3A). Total Bcl-xL level remained stable along mitosis. Interestingly, the Bcl-xL(Ser49) phosphorylation pattern was exactly opposite that of Bcl-xL(Ser62) (Fig. 3A), indicating differential function. CyclinB1 and phospho-H3(Ser10) expression is shown as a specific early mitotic phase marker (Fig. 3A). The location of phospho-Bcl-xL(Ser49) in telophase/cytokinesis was then investigated. In these experiments, HeLa cells were synchronized by double thymidine block and release upon progression to G2 and entry into mitosis. They

were collected at 30-min intervals from 9 to 12 h after double thymidine block and release to acquire mitotic cells at all steps of mitosis. In telophase/cytokinesis, phospho-Bcl-xL(Ser49) co-localizes with the microtubule associated motor protein dynein (Fig. 3B). Phospho-Bcl-xL(Ser49) does not localize in centrosomes with γ-tubulin in telophase/cytokinesis (Fig. 3B). A summary of microscopy analysis is presented in Supplemental Table S1.

3.4. Polo kinase 3 (PLK3) is involved in Bcl-xL(Ser49) phosphorylation

To identify the putative protein kinase involved in Bcl-xL(Ser49) phosphorylation, a panel of protein kinases was first tested in in vitro kinase assays with recombinant human Bcl-xL protein as substrate. Among all the kinases tested, PLK3 was the only one able to phosphorylate recombinant Bcl-xL protein on Ser49 in in vitro kinase assays (Fig. 4A). Enzyme-specific activities with control substrates are illustrated in Supplemental Fig. S3-A–B. The specificity of Ser49 phosphorylation by PLK3 was validated by mass spectrometry (Supplemental Fig. S3-C). PLK3 participation in Bcl-xl(Ser49) phosphorylation during DNA damage-induced G2 arrest was validated by deploying 2 specific small interfering RNAs (siRNAs) targeting PLK3 mRNA. A schematic illustration of these experiments appears in Fig. 4B.

With siRNAs targeting PLK3 mRNA, several attempts were made to confirm its involvement in Bcl-xL(Ser49) phosphorylation at telophase/cytokinesis (data not reported). Interfering with PLK3 expression does not allow cells to undergo proper cytokinesis, with most cells been blocked at G2 or harboring a multinucleated phenotypes, effects reported previously by expressing death kinase mutant enzymes, or in cells exposed to PLK3 shRNA [58–61]. Trying to circumvent it, we adopted a protocol similar to that described in Fig. 3, where synchronized cells at G2 are first allowed to accumulate at metaphase with nocodazole, then released in the presence of blebbistatin to enrich the cell population at telophase/cytokinesis. A fraction of the cells was released from nocodazole and then treated with blebbistatin with or without BI-2536, a PLK inhibitor. The cells were also collected by mitotic shake-off to avoid the presence of multinucleated cells. The experiments are illustrated schematically in Fig. 4C. Inhibiting PLK activities in these cells prevented Bcl-xL(Ser49) phosphorylation. However, they also failed to enter telophase/cytokinesis as cyclin B1 and phospho-H3(Ser10) expression remained significantly high. Together, these experiments confirmed that cytokinesis requires PLK3 activity. Quenching its expression with siRNAs or suppressing its activity in a timely manner in synchronized cells after nocodazole release causes cytokinesis defects, which also correlate with failure to phosphorylate Bcl-xL (Ser49).

4. Discussion

This study reveals a new phosphorylation site within Bcl-xL – Bcl-xL (Ser49) – that undergoes dynamic phosphorylation/dephosphorylation events during cell cycle progression. Phospho-Bcl-xL(Ser49) is essential in at least 2 key events of the cell cycle, G2 checkpoint and progression to telophase/cytokinesis during mitosis. A pool of phospho-Bcl-xL(Ser49) strongly localizes at centrosomes with γ-tubulin during the G2 checkpoint induced by DNA damage, and with the microtubule associated dynein motor protein during telophase/

cytokinesis. PLK3, which has known essential functions during cell cycle progression, is a key kinase involved in Bcl-xL(Ser49) phosphorylation. Importantly, phospho-Bcl-xL(Ser49) functions during G2 checkpoint and, in mitosis, it appears to be separable from Bcl-xL's known role in apoptosis, as Bcl-xL (Ser49Ala) phosphorylation mutant retains its anti-apoptotic effect but clearly shows different cell cycle behavior in DNA damage-induced G2 arrest and taxol-mediated mitotic actions.

Bcl-xL phosphorylation at Ser62 is well-documented and generally associated with microtubule poisoning [41–49]. Phospho-Bcl-xL(Ser62) functions have remained elusive until recently. We currently observed that it undergoes differential location during G2 and spindle-assembly checkpoints (Wang et al., 2011; manuscripts submitted). A pool of phospho-Bcl-xL(Ser 62) is located in Cajal bodies in interphase and a pool accumulates with CDK1(CDC2) in nucleoli during G2 checkpoint, whereas its interacts with the inhibitory CDC20/MAD2/BUBR1/BUB3 complex during spindle-assembly checkpoints (Wang et al., 2011; manuscripts submitted). Interestingly, in this study, we noted a differential pattern of expression and location for phospho-Bcl-xL (Ser49) compared to phospho-Bcl-xL(Ser62). Phospho-Bcl-xL(Ser49) accumulates in centrosomes during G2 checkpoint, is rapidly dephosphorylated at early mitotic phases and is re-phosphorylated during telophase/cytokinesis. These dynamic changes of location and phosphorylation/dephosphorylation events strongly indicate differential functions. Although the exact molecular mechanisms were not fully addressed here, functional changes in cell cycle progression and cell behavior in response to VP16 and taxol treatment are documented, with cells expressing the Bcl-xL(Ser49Ala) phosphorylation mutant.

PLK3 activity and function have been reviewed recently [62]. Observed in centrosomes and nucleoli during interphase [60,63], PLK3 is found at spindle poles and midbody during cytokinesis [59,60]. PLK3 activity increases rapidly after DNA damage in an ATM-dependent manner, and is involved in G2 arrest by phosphorylating and inhibiting CDC25C phosphatase [64–67]. Its exact functions during mitosis remain unclear, but overexpression of PLK3's polo box domain, but not the kinase domain, causes cytokinesis defects, aneuploidy and cell death [58–60]. Similarly, cells harboring PLK3 knockdown by small hairpin RNA presented incomplete cytokinesis, which produced a fair amount of multinucleated cells [61]. PLK3 strongly phosphorylated Bcl-xL(Ser49) in in vitro kinase assays. RNA interference experiments conducted during G2 arrest confirmed that PLK3 is the key enzyme in Bcl-xL(Ser49) phosphorylation. During cytokinesis, our results are strongly indicative of PLK3's involvement, having demonstrated correlations between PLK3 expression and activity, failure to enter cytokinesis and to phosphorylate Bcl-xL at Ser49. The functional outcome of phospho-Bcl-xL(Ser49) on the stability of G2 checkpoint and kinetics of cytokinesis also correlates with PLK3 functions during G2 arrest and cytokinesis, suggesting that Bcl-xL is a downstream target of PLK3 and part of the network mediating PLK3's effect.

In summary, our data disclose a yet uncharacterized phosphorylation site within Bcl-xL. Bcl-xL(Ser49) is phosphorylated during normal cell cycle progression and checkpoints. Interfering with Bcl-xL (Ser49) phosphorylation destabilizes DNA damage-induced G2 arrest and slows entry into cytokinesis, but has no effect on the kinetics of VP16- and taxol-

induced apoptosis. Our data also indicate that PLK3 is involved in Bcl-xL(Ser49) phosphorylation at G2 checkpoint and cytokinesis. Additional work is underway to dissect the molecular mechanisms of phospho-Bcl-xL(Ser49) action.

Supplementary Material

Refer to Web version on PubMed Central for supplementary material.

Acknowledgments

This work was supported by Grant MOP-97913 from the Canadian Institutes of Health Research to R.B. J.W. received scholarships from the China Scholarship Council (Beijing, China), the Faculté des études supérieures (Université de Montréal, Canada) and the Fondation de l'Institut du cancer de Montréal (Canada). The authors thank Dr. Estelle Schmitt (CRCHUM, Canada) for her valuable suggestions and the preparation of Bcl-xL mutant cDNAs, and Dr. Guy G. Poirier (CRCHUL, Canada) for MS/MS analysis. The editorial work of Mr. Ovid Da Silva is appreciated.

Abbreviations

Bcl	B cell leukemia/lymphoma protein
Bcl-xL	Bcl-2-related gene x, long isoform
BH	Bcl-2 homology domain
CDC	cell division cycle
CDK	cyclin dependent kinase
CLIP170	cytoplasmic linker protein 170
HA	influenza hemagglutinin epitope tag
PCR	polymerase chain reaction
PI	propidium iodide
PLK	polo kinase
siRNA	small interfering RNA
VP16	etoposide
wt	wild-type

References

1. Boise LH, Gonzalez-Garcia M, Postema CE, Ding L, Lindsten T, Turka LA, et al. Cell. 1993; 74:597. [PubMed: 8358789]
2. Paquet, C., Bertrand, R. Recent Research Developments in Biophysics and Biochemistry. Gayathri, A., editor. Research Signpost Publisher; Trivandrum: 2003. p. 291
3. Kroemer G, Galluzzi L, Brenner C. Physiol Rev. 2007; 87:99. [PubMed: 17237344]
4. Tait SW, Green DR. Nat Rev Mol Cell Biol. 2010; 11:621. [PubMed: 20683470]
5. Muchmore SW, Sattler M, Liang H, Meadows RP, Harlan JE, Yoon HS, et al. Nature. 1996; 381:335. [PubMed: 8692274]

6. Sattler M, Liang H, Nettesheim D, Meadows RP, Harlan JE, Eberstadt M, et al. Science. 1997; 275:983. [PubMed: 9020082]
7. Diaz JL, Oltersdorf T, Horne W, McConnell M, Wilson G, Weeks S, et al. J Biol Chem. 1997; 272:11350. [PubMed: 9111042]
8. Sedlak TW, Oltvai ZN, Yang E, Wang K, Boise LH, Thompson CB, et al. Proc Nat Acad Sci USA. 1995; 92:7834. [PubMed: 7644501]
9. Cheng EH, Wei MC, Weiler S, Flavell RA, Mak TW, Lindsten T, et al. Mol Cell. 2001; 8:705. [PubMed: 11583631]
10. Letai A, Bassik M, Walensky L, Sorcinelli M, Weiler S, Korsmeyer S. Cancer Cell. 2002; 2:183. [PubMed: 12242151]
11. Kuwana T, Bouchier-Hayes L, Chipuk JE, Bonzon C, Sullivan BA, Green DR, et al. Mol Cell. 2005; 17:525. [PubMed: 15721256]
12. Certo M, Del Gaizo Moore V, Nishino M, Wei G, Korsmeyer S, Armstrong SA, et al. Cancer Cell. 2006; 9:351. [PubMed: 16697956]
13. Willis SN, Fletcher JI, Kaufmann T, van Delft MF, Chen L, Czabotar PE, et al. Science. 2007; 315:856. [PubMed: 17289999]
14. Adams JM, Cory S. Curr Opin Immunol. 2007; 19:488. [PubMed: 17629468]
15. Youle RJ, Strasser A. Nat Rev Mol Cell Biol. 2008; 9:47. [PubMed: 18097445]
16. Chittenden T. Cancer Cell. 2002; 2:165. [PubMed: 12242145]
17. Lovell JF, Billen LP, Bindner S, Shamas-Din A, Fradin C, Leber B, et al. Cell. 2008; 135:1074. [PubMed: 19062087]
18. Kim H, Tu HC, Ren D, Takeuchi O, Jeffers JR, Zambetti GP, et al. Mol Cell. 2009; 36:487. [PubMed: 19917256]
19. Dewson G, Kluck RM. J Cell Sci. 2009; 122:2801. [PubMed: 19795525]
20. Gavathiotis E, Reyna DE, Davis ML, Bird GH, Walensky LD. Mol Cell. 2010; 40:481. [PubMed: 21070973]
21. Minn AJ, Velez P, Schendel SL, Liang H, Muchmore SW, Fesik SW, et al. Nature. 1997; 385:353. [PubMed: 9002522]
22. Zoratti M, Szabo I. Biochim Biophys Acta. 1995; 1241:139. [PubMed: 7640294]
23. Shimizu S, Narita M, Tsujimoto Y. Nature. 1999; 399:483. [PubMed: 10365962]
24. Harris MH, Thompson CB. Cell Death Differ. 2000; 7:1182. [PubMed: 11175255]
25. Shimizu S, Konishi A, Kodama T, Tsujimoto Y. Proc Nat Acad Sci USA. 2000; 97:3100. [PubMed: 10737788]
26. Shimizu S, Shinohara Y, Tsujimoto Y. Oncogene. 2000; 19:4309. [PubMed: 10980606]
27. Kroemer G, Reed JC. Nat Med. 2000; 6:513. [PubMed: 10802706]
28. Zamzami N, Kroemer G. Nat Rev Mol Cell Biol. 2001; 2:67. [PubMed: 11413468]
29. Pavlov EV, Priault M, Pietkiewicz D, Cheng EH, Antonsson B, Manon S, et al. J Cell Biol. 2001; 155:725. [PubMed: 11724814]
30. Qian S, Wang W, Yang L, Huang HW. Proc Nat Acad Sci USA. 2008; 105:17379. [PubMed: 18987313]
31. Yamaguchi R, Lartigue L, Perkins G, Scott RT, Dixit A, Kushnareva Y, et al. Mol Cell. 2008; 31:557. [PubMed: 18691924]
32. Schmitt E, Paquet C, Beauchemin M, Bertrand R, Zhejiang J. Univ Sci B. 2007; 8:377.
33. Danial NN, Gimenez-Cassina A, Tondera D. Adv Exp Med Biol. 2010; 687:1. [PubMed: 20919635]
34. Saintigny Y, Dumay A, Lambert S, Lopez BS. EMBO J. 2001; 20:2596. [PubMed: 11350949]
35. Wang Q, Gao F, May WS, Zhang Y, Flagg T, Deng X. Mol Cell. 2008; 29:488. [PubMed: 18313386]
36. Wiese C, Pierce AJ, Gauny SS, Jasin M, Kronenberg A. Cancer Res. 2002; 62:1279. [PubMed: 11888891]
37. Youn CK, Cho HJ, Kim SH, Kim HB, Kim MH, Chang IY, et al. Nat Cell Biol. 2005; 7:137. [PubMed: 15619620]

38. Janumyan YM, Sansam CG, Chattopadhyay A, Cheng N, Soucie EL, Penn LZ, et al. EMBO J. 2003; 22:5459. [PubMed: 14532118]
39. Janumyan Y, Cui Q, Yan L, Sansam CG, Vanlentin M, Yang E. J Biol Chem. 2008; 283:34108. [PubMed: 18818203]
40. Schmitt E, Beauchemin M, Bertrand R. Oncogene. 2007; 26:5851. [PubMed: 17369848]
41. Poruchynsky MS, Wang EE, Rudin CM, Blagosklonny MV, Fojo T. Cancer Res. 1998; 58:3331. [PubMed: 9699663]
42. Fang GF, Chang BS, Kim CN, Perkins C, Thompson CB, Bhalla KN. Cancer Res. 1998; 58:3202. [PubMed: 9699642]
43. Johnson AL, Bridgham JT, Jensen T. Endocrinology. 1999; 140:4521. [PubMed: 10499507]
44. Fan M, Du C, Stone AA, Gilbert KM, Chambers TC. Cancer Res. 2000; 60:6403. [PubMed: 11103805]
45. Basu A, Haldar S. FEBS Lett. 2003; 538:41. [PubMed: 12633850]
46. Du L, Lyle CS, Chambers TC. Oncogene. 2005; 24:107. [PubMed: 15531923]
47. Upreti M, Galitovskaya EN, Chu R, Tackett AJ, Terrano DT, Granell S, et al. J Biol Chem. 2008; 283:35517. [PubMed: 18974096]
48. Tamura Y, Simizu S, Muroi M, Takagi S, Kawatani M, Watanabe N, et al. Oncogene. 2009; 28:107. [PubMed: 18820703]
49. Terrano DT, Upreti M, Chambers TC. Mol Cell Biol. 2010; 30:640. [PubMed: 19917720]
50. Kharbanda S, Saxena S, Yoshida K, Pandey P, Kaneki M, Wang Q, et al. J Biol Chem. 2000; 275:322. [PubMed: 10617621]
51. Chang BS, Minn AJ, Muchmore SW, Fesik SW, Thompson CB. EMBO J. 1997; 16:968. [PubMed: 9118958]
52. Srivastava RK, Mi QS, Hardwick JM, Longo DL. Proc Nat Acad Sci USA. 1999; 96:3775. [PubMed: 10097113]
53. Andreassen PR, Skoufias DA, Margolis RL. Methods Mol Biol. 2004; 281:213. [PubMed: 15220532]
54. Loffler H, Lukas J, Bartek J, Kramer A. Exp Cell Res. 2006; 312:2633. [PubMed: 16854412]
55. Jackman M, Lindon C, Nigg EA, Pines J. Nat Cell Biol. 2003; 5:143. [PubMed: 12524548]
56. Kramer A, Mailand N, Lukas C, Syljuasen RG, Wilkinson CJ, Nigg EA, Bartek J, Lukas J. Nat Cell Biol. 2004; 6:884. [PubMed: 15311285]
57. Schmitt E, Boutros R, Froment C, Monsarrat B, Ducommun B, Dozier C. J Cell Sci. 2006; 119:4269. [PubMed: 17003105]
58. Conn CW, Hennigan RF, Dai W, Sanchez Y, Stambrook PJ. Cancer Res. 2000; 60:6826. [PubMed: 11156373]
59. Wang Q, Xie S, Chen J, Fukasawa K, Naik U, Traganos F, et al. Mol Cell Biol. 2002; 22:3450. [PubMed: 11971976]
60. Jiang N, Wang X, Jhanwar-Uniyal M, Darzynkiewicz Z, Dai W. J Biol Chem. 2006; 281:10577. [PubMed: 16478733]
61. Naik MU, Naik UP. Int J Biochem Cell Biol. 2011; 43:120. [PubMed: 20951827]
62. Strebhardt K. Nat Rev Drug Discovery. 2010; 9:643. [PubMed: 20671765]
63. Zimmerman WC, Erikson RL. Proc Nat Acad Sci USA. 2007; 104:1847. [PubMed: 17264206]
64. Xie S, Wu H, Wang Q, Cogswell JP, Husain I, Conn C, et al. J Biol Chem. 2001; 276:43305. [PubMed: 11551930]
65. Bahassi EM, Conn CW, Myer DL, Hennigan RF, McGowan CH, Sanchez Y, et al. Oncogene. 2002; 21:6633. [PubMed: 12242661]
66. Myer DL, Bahassiel M, Stambrook PJ. Oncogene. 2005; 24:299. [PubMed: 15640846]
67. Bahassi EM, Myer DL, McKenney RJ, Hennigan RF, Stambrook PJ. Mutat Res. 2006; 596:166. [PubMed: 16481012]

Appendix A. Supplementary data

Supplementary data to this article can be found online at doi:10. 1016/j.cellsig.2011.07.017.

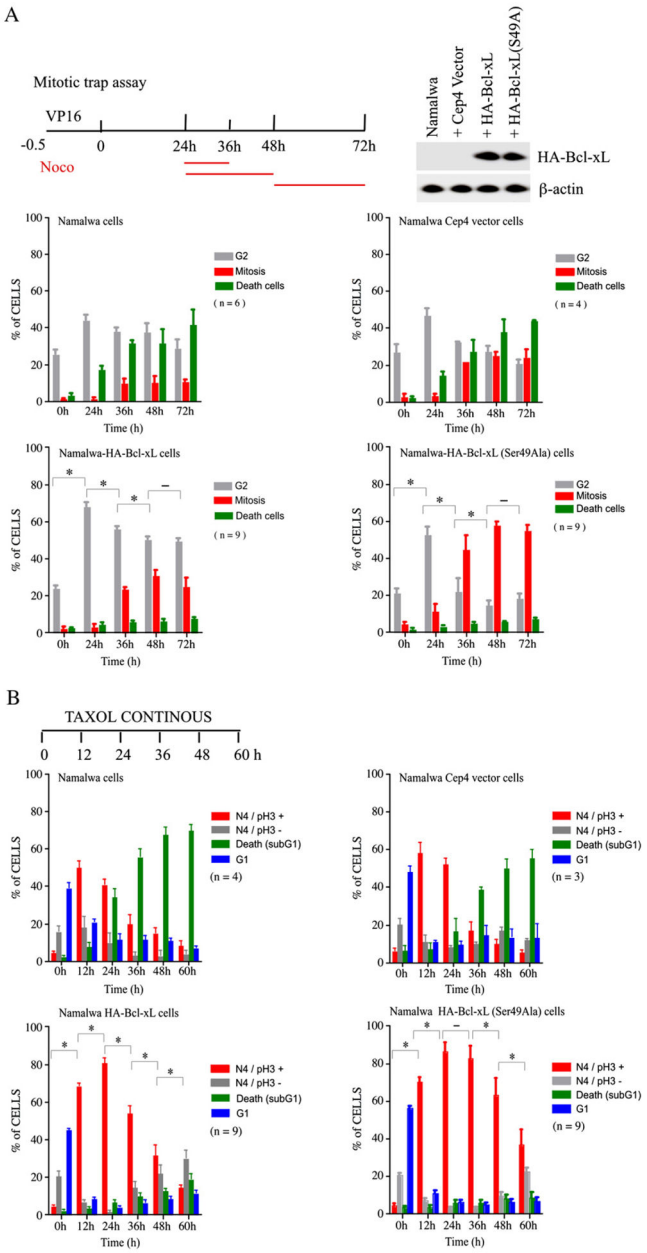

Fig. 1.

Effect of Bcl-xL and Bcl-xL(Ser49Ala) phosphorylation mutant on G2 checkpoint resolution and entry into cytokinesis. A) G2 checkpoint experiments are illustrated schematically in the top left panel. The expression levels of HA-Bcl-xL, HA-Bcl-xL(Ser49Ala) phosphorylation mutant and β-actin in stably-transfected Namalwa cell populations are shown in the top right panel. Kinetics of G2 cells (N4 DNA content, phospho-H3(Ser10)-negative; gray bars), early mitotic cells (N4 DNA content, phospho-H3(Ser10)-positive) and dead cells (sub-G1 cells; green bars) in wt Namalwa cells and Namalwa cells expressing empty vector, HA-Bcl-xL and HA-Bcl-xL(Ser49Ala) phosphorylation mutant after VP16 treatment. Bars represent the means±s.e.m. of *n* independent experiments. Statistical analysis are showed for G2 cells

(gray bars) in Namalwa cells expressing HA-Bcl-xL and HA-Bcl-xL(Ser49Ala) phosphorylation mutant. * Significant ($p<0.05$); – non-significant ($p>0.05$). B) Taxol experiments are illustrated schematically in the top left. Kinetics of early mitotic cells (N4 DNA content, phospho-H3(Ser10)-positive; red bars), late mitotic cells (or G2 at time 0) (N4 DNA content, phospho-H3(Ser10)-negative; gray bars), dead cells (sub-G1 cells; green bars) and G1 cells (N2 DNA content; blue bars) in wt Namalwa cells and Namalwa cells expressing empty vector, HA-Bcl-xL and HA-Bcl-xL(Ser49Ala) phosphorylation mutant during taxol treatment (0.1 μM). Bars represent the means±s.e.m. of *n* independent experiments. Statistical analysis are showed for early mitotic cells (red bars) in Namalwa cells expressing HA-Bcl-xL and HA-Bcl-xL(Ser49Ala) phosphorylation mutant. * Significant ($p<0.05$); – non-significant ($p>0.05$).

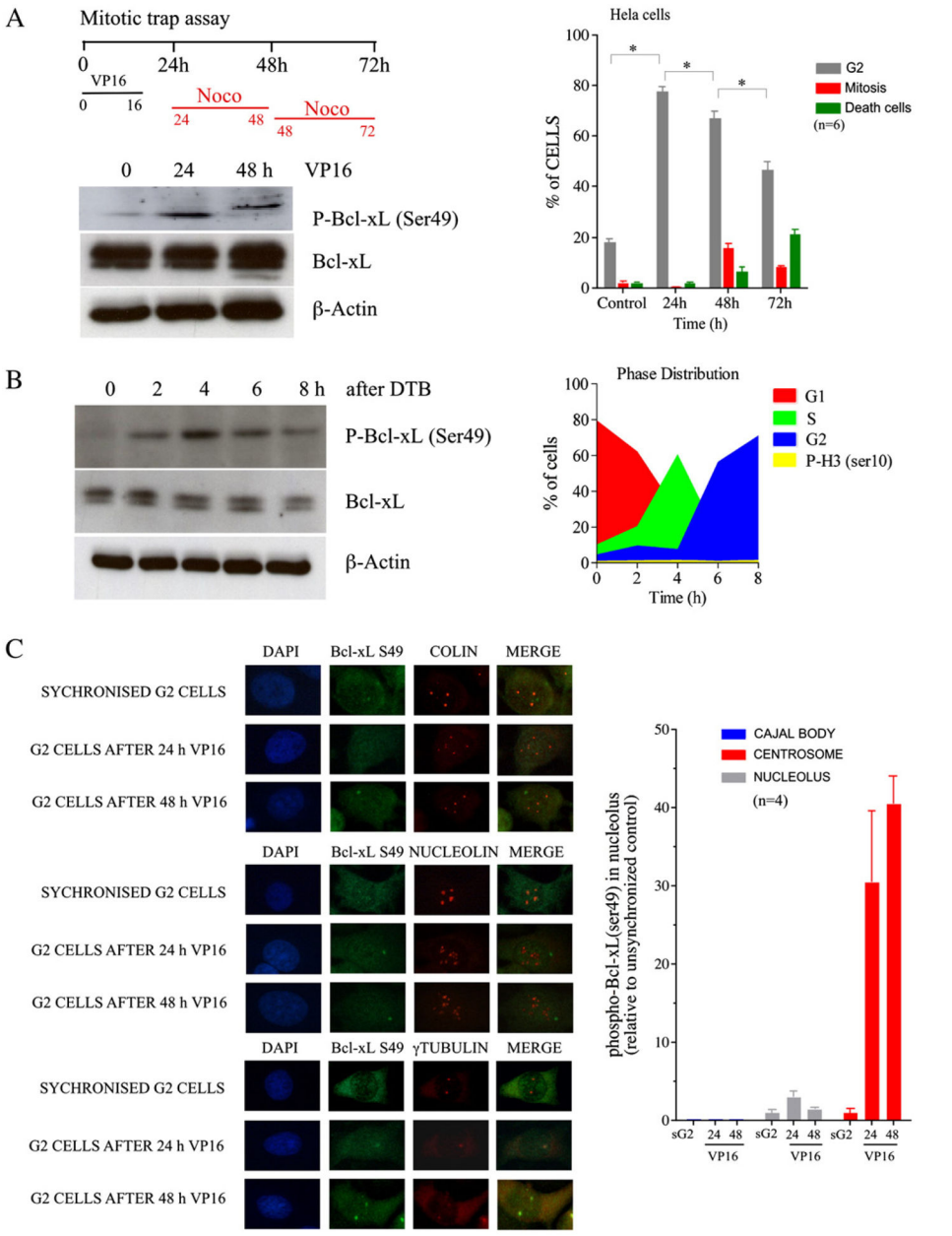

Fig. 2.

Bcl-xL(Ser49) phosphorylation and location during DNA damage-induced G2 arrest and in unpertubed, synchronized wt Hela cells at interphase. A) Expression kinetics of phospho-Bcl-xL(Ser49), Bcl-xL and β-actin in wt HeLa cells treated with VP16. These experiments are illustrated schematically at the top. Kinetics of G2 cells (N4 DNA content, phospho-H3(Ser10)-negative; gray bars), early mitotic cells (N4 DNA content, phospho-H3(Ser10)-positive; red bars) and dead cells (sub-G1 cells; green bars) in wt HeLa cells treated with VP16 appear on the right histogram. Bars represent the means±s.e.m. of *n* independent experiments. Statistical analysis are showed for G2 cells (gray bars); * Significant ($p<0.05$). B) Expression kinetics of phospho-Bcl-xL(Ser49), Bcl-xL and β-actin in synchronized HeLa cells after double-thymidine block release. Cell cycle phase distribution during these

experiments is illustrated in the right histogram. C) Co-location of phospho-Bcl-xL(Ser49) with colin (Cajal body markers), nucleolin (nucleolus marker) and γ-tubulin (centrosome marker) in synchronized G2 cells and during VP16-induced DNA damage and G2 arrest. The percentages of phospho-Bcl-xL(Ser49) in nucleoli, Cajal bodies and centrosomes during VP16-induced G2 checkpoint and during normal G2 phase of the cell cycle in synchronized wt Hela cells (sG2) are indicated in the right histogram. Bars represent the means±s.e.m. from micrographs obtained in 4 independent experiments.

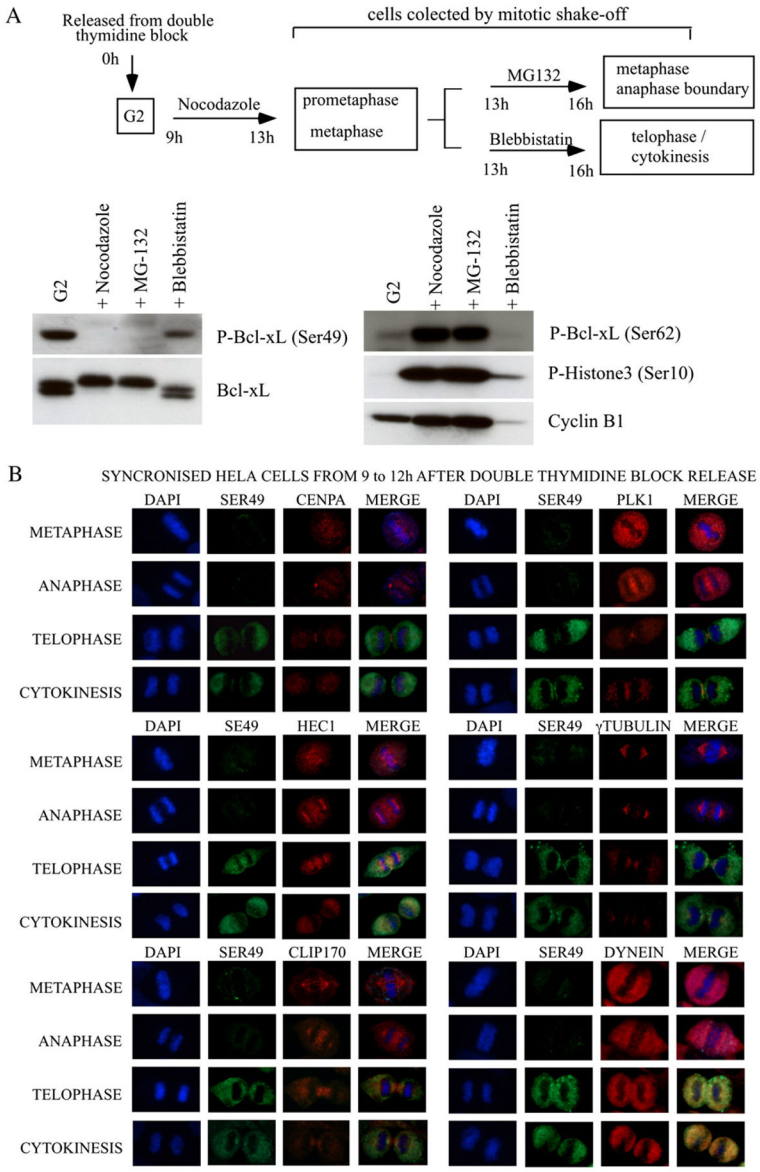

Fig. 3.

Bcl-xL(Ser49) phosphorylation and location during mitosis progression. A) Expression kinetics of phospho-Bcl-xL(Ser49), phospho-Bcl-xL(Ser62), Bcl-xL, phospho-H3(Ser10) and cyclin B1 in wt HeLa cells obtained at different steps of mitosis. The design of these experiments is illustrated at the top. B) Co-location of phospho-Bcl-xL(Ser49) with dynein motor protein in telophase/cytokinesis. Representative of a total of 624 cells obtained from 3 experiments. Details in Supplemental Table S1.

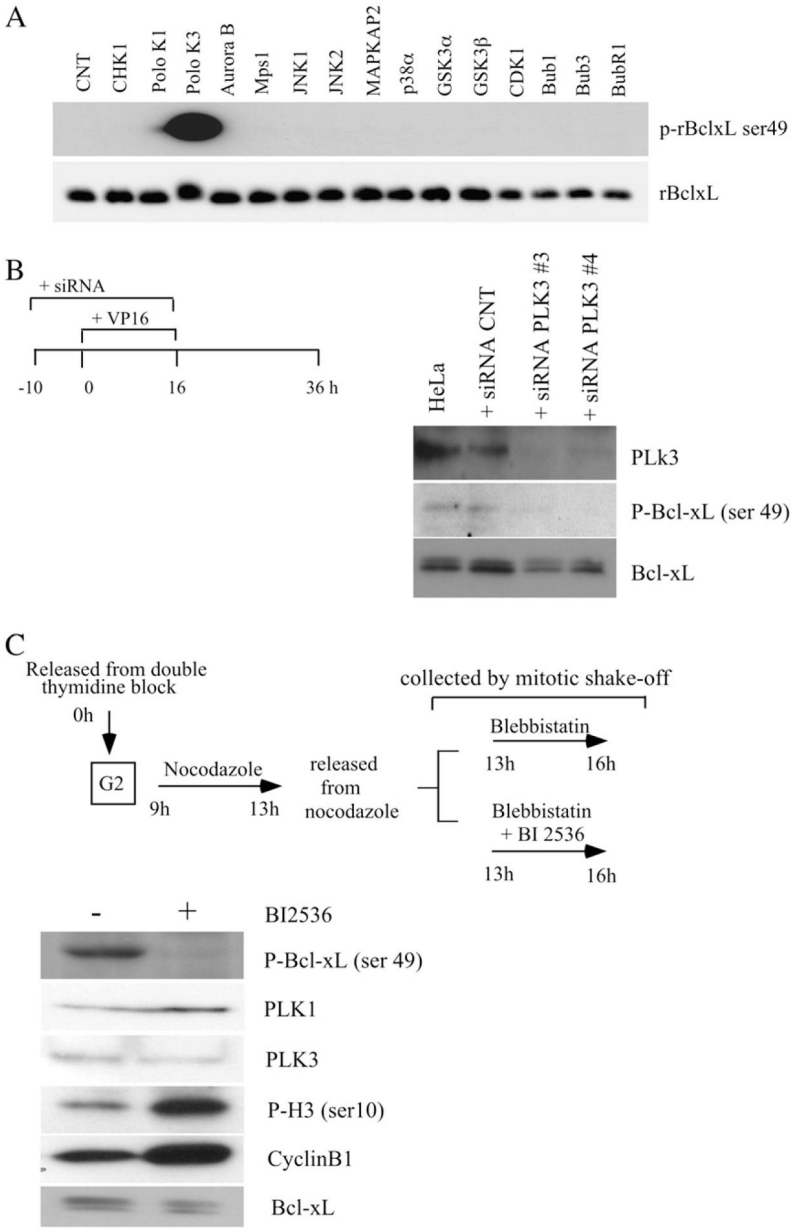

Fig. 4.

PLK3 is involved in Bcl-xL(Ser49) phosphorylation. A) In vitro assays of a panel of purified and active protein kinases with recombinant human Bcl-xL(ΔTM) protein as substrate. All enzyme activities were tested on control substrates in Supplemental Fig. S3-A–B, and validation by mass spectrometry appears in Supplemental Fig. S3-C. Western blots are representative of 3 independent experiments. B) Effects of 2 specific siRNAs targeting PLK3 mRNA on the expression kinetics of phospho-Bcl-xL(Ser49), Bcl-xL and PLK3 in wt HeLa cells exposed to VP16. The design of these experiments is presented on the left. C) Effects of a PLK inhibitor (BI-2536, 0.1 μm) on phospho-Bcl-xL(Ser49), Bcl-xL, PLK1 and PLK3 expression in synchronized wt HeLa cells released from nocodazole in the presence of

blebbistatin to obtain enriched telophase/cytokinesis. The design of these experiments is presented at the top. Western blots are representative of 2 independent experiments.